[EA]Thermo-Tectono-Stratigraphic Modelling of a Northern Red Sea Transect and Implications for the Petroleum Systems*

T.A. Cunha[1], P. Baptista[2], L.H. Rüpke[3], D.W. Schmid[3], I. Davison[4], and R. Bertolotti[2]

Search and Discovery Article #30666 (2020)**
Posted June 15, 2020

*Extended abstract adapted from oral presentation given at 2020 AAPG Middle East Region, Rift Basin Evolution and Exploration GTW: The Global State of the Art and Applicability to the Middle East and Neighbouring Regions, Bahrain, February 3-5, 2020
 DOI:10.1306/30666Cunha2020

[1]IGI Ltd. Hallsannery, Bideford, United Kingdom (tiago@igiltd.com)
[2]Mubadala Petroleum, Abu Dhabi
[3]GeoModelling Solutions GmbH, Zurich, Switzerland
[4]Earthmoves Ltd., Camberley, United Kingdom

Abstract

The Red Sea is an active rift system that initiated in the late Oligocene between the Arabian and Africa plates. Hydrocarbon exploration in the Red Sea has focused largely in the northern, shallow water Gulf of Suez region, where more than 1500 exploration wells have been drilled since the 1880's, resulting in numerous discoveries and estimated reserves in excess of 12 bboe (Wescott et al., 2016). Several discoveries have also been reported along the southern Red Sea, namely offshore Sudan and Eritrea (Lindquist, 1998). Together with widespread seeps and shows (Lindquist, 1998; Dolson, 2018), these suggest working petroleum systems in the region, and a recent license round covering most of the Egyptian Red Sea attracted several major oil and gas exploration companies.

In this study, we apply a thermo-tectono-stratigraphic basin reconstruction modelling technique (TecMod-2D) to a seismic transect in the northern sector of the Red Sea, extending between the western (Egyptian) margin and the rift axis. The model solves simultaneously for basin-scale (e.g. sedimentation, compaction) and lithosphere-scale (e.g. crust/mantle thinning, break-up, flexure, mantle serpentinization) processes, and iteratively inverts for the stratigraphy, varying the sedimentation rates and paleowater depths (Rüpke et al., 2008). The modelling provides self-consistent thermal and burial histories for a given lithosphere parameterization, rift history and stratigraphic input, and is a powerful tool in frontier rift basins. By varying key modelling inputs, and calibrating the model predictions to observations/measurements on the structure of the lithosphere and present-past thermal regimes, we are able to put constraints on the basin-forming processes and evaluate their implications for the known (and speculative) petroleum systems.

Summary of Results and Discussion

1. The burial history of the margin is successfully reproduced for reasonable model boundary conditions, where the age of the late Oligocene-early Miocene rifting is defined based on regional tectonic studies, integrating the basins' stratigraphy, the age of volcanic events and structural analysis (e.g. Bosworth et al., 2005; and references therein), and the structure of the pre-rift lithosphere is constrained from seismic receiver function techniques (Hansen et al., 2007; Hosny and Nyblade, 2016; Figure 1a).

2. The high heat flow observed along the Red Sea is modelled (Figure 1c) for active rifting since the mid/late Miocene (no crustal stretching). The models are calibrated to the temperature data available at four well locations (Figure 1b), located to the north and south of the profile (see map in Figure 1a), and are consistent with a shallow asthenosphere-lithosphere boundary (LAB) centered in the Red Sea at < 50 km depth (Figure 1d), as inferred from combined S-wave receiver function and gravity modelling techniques (Hansen et al., 2007). The models also recover a Moho depth of 10-12 km near the axis of the Red Sea (Figure 1e), consistent with seismic velocity and gravity models (Gaulier et al., 1988; Hansen et al., 2007).

3. A large number of modelling scenarios have been tested, varying the structure and thermal properties of the crust/lithosphere, the parameterization of the initial (passive) and mid Miocene onwards (active) rift events, the thermal properties of sediments and timing/duration of salt deposition. Within reasonable uncertainty, and considering the calibration to the available temperature and heat flow data, as well as the constraints on the structure of the lithosphere, the models predict the present-day heat flow at the base of the sediments to vary between 70 and 110 $mW.m^2$ (Figure 1c).

4. The models predict the depth of the main oil window to vary broadly between burial depths of 3.5 to 4 km in the west, near the Egyptian margin, and 4 to 4.5 km towards the rift axis (Figure 2a). These depths are similar to those reported by Dolson (2018) in the Gulf of Suez, in somewhat cooler geothermal gradients (and lower average surface heat flow values), but with a thinner Miocene salt coverage (Rohais et al., 2016).

5. The modelling results further suggest that oil maturity of the deeper syn-rift horizons, and potential pre-rift source rocks takes place from the mid Miocene onwards, followed by gas generation in the deeper grabens (Figure 2c), while the shallower pre-salt horizons are likely to generate oil from the late Miocene onwards (Figure 2b). Recent gas expulsion from the deeper horizons could significantly improve the basin prospectivity, by generating sufficient volumes for efficient secondary oil migration, which can locally reach the surface (e.g. seeps in the vicinity of the rift axis). The variations in the predicted maturity and timings of oil and gas generation between the reference and the hotter and colder end-member models (see Figure 1c) is relatively small; less than 500 m and 5 Ma in the depth and timing of the oil and gas windows, respectively.

6. We also tested the impact of mantle serpentinization and oceanization in the predicted heat flow and basin maturity. Allowing for serpentinization of the upper mantle (up to 40% mantle serpentinization with as little as 80% of crust embrittlement) raises the syn-rift (Oligocene-mid Miocene) heat flow by as much as 30-40 $mW.m^2$ in some sections of the profile (see Rüpke et al., 2013 for modelling serpentinization in TecMod-2D, and brief description of causes and consequences), but does have a significant impact on the predicted depth-

timing of maturity of the potential syn- and pre-rift source rock horizons. If the creation of new oceanic crust is considered, assuming break-up at approximately 45 km along the profile during the mid-Miocene (end-member model), then the pre-rift and break-up sediment sequences, if existent, would be over-mature under the allochthonous salt, but the predicted basin maturity in the large half-grabens to the west is not significantly affected.

References Cited

Bosworth W., P. Huchon and K. McClay, 2005, The Red Sea and Gulf of Aden basins: Journal of African Earth Sciences, v. 43, p. 334–378.

Dolson, J., 2018, What Will it Take to Bring a Renaissance to Gulf of Suez Exploration: Has the Time Arrived to Try Some Unconventional Source Rock Plays?: Search and Discovery Article #11153, Web Accessed May 31, 2020.

Gaulier, J.M, X. Le Pichon, N. Lyberis, F. Avedik, L. Gel, I. Moretti, A. Deschamps and S. Hafez, 1988, Seismic study of the crust of the northern Red Sea and Gulf of Suez: Tectonophysics, v. 153, p. 55-88.

GEBCO Compilation Group (2019) GEBCO 2019 Grid (doi:10.5285/836f016a-33be-6ddc-e053-6c86abc0788e).

Hansen, S. E., A. J. Rodgers, S.Y. Schwartz and A.M.S. Al-Amri, 2007, Imaging ruptured lithosphere beneath the Red Sea and Arabian Peninsula: Earth and Planetary Science Letters, v. 259, p. 256-265.

Hosny, A. and A. Nyblade, 2016, The crustal structure of Egypt and the northern Red Sea region: Tectonophysics, v. 687, p. 257-267.

IHFC the International Heat Flow Commission (http://ihfc-iugg.org/).

Lindquist, S.J., 1998, The Red Sea Basin Province: Sudr-Nubia(!) and Maqna(!) Petroleum Systems: U.S. Geological Survey, Open-file Report 99-50-A.

Rohais, S., A. Barrois, C. Colletta and I. Moretti, 2016, Pre-salt to salt stratigraphic architecture in a rift basin: insights from a basin-scale study of the Gulf of Suez (Egypt): Arabian Journal of Geosciences, Springer, v. 9, 10.1007/s12517-016-2327-8.

Rüpke, L.H., S.M. Schmalholz, D.W. Schmid, and Y.Y. Podiadchikov, 2008, Automated thermo-tectonostratigraphic basin reconstruction: Viking Graben case study: AAPG Bulletin, v. 92, p. 309-326.

Rüpke, L.H., D.W. Schmid, and E.H. Hartz, 2013, Causes and consequences of mantle serpentinization during passive margin formation: Search and Discovery Article #120118, Web Accessed May 31, 2020.

Sweeney, J.J. and A.K. Burnham, 1990, Evaluation of a simple model of vitrinite reflectance based on chemical kinetics: AAPG Bulletin, v. 74, p. 1559–1570.

Wescott, W.A., M. Atta and J.C. Dolson, 2016, Brief History of the Exploration History of the Gulf of Suez, Egypt: Search and Discovery Article #30473, Web Accessed May 31, 2020.

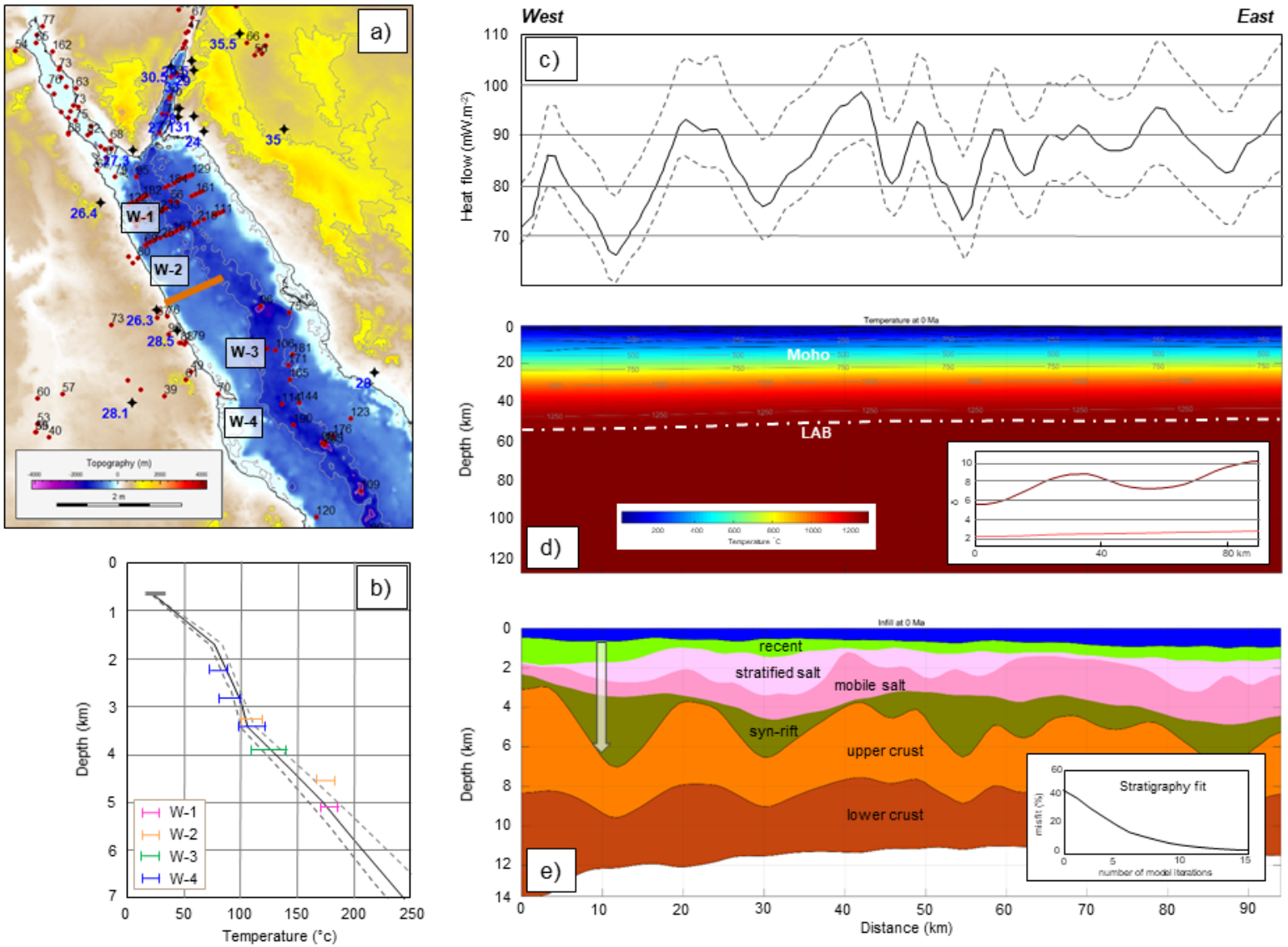

Figure 1. a) Topography-bathymetric map of the central-northern Red Sea and Gulf of Suez/Gulf of Aqaba region (GEBCO, 2019), showing the approximate location of the modelled transect (thick orange line), heat flow (HF) measurements from the International Heat Flow Commission (IHFC; www.ihfc-iugg.org) database (red dots, with representative values in black), Moho depths (in dark blue) from Hosny and Nyblade (2016; joint inversion of P-wave receiver functions and Rayleigh wave group velocities) and Hansen et al. (2007; S-wave receiver functions), and the approximate location of four wells (W-1,2,3,4; white-transparent rectangles) where we have temperature measurements from wireline logs for calibration. *(Continued on next slide)*

(Continued from previous slide)

b) Temperature-depth plots for three models covering the variability in the geothermal gradients in the area inferred from the borehole data. The reference model (solid black line) assumes a 28 km thick crust overlying a 100 km thick mantle lithosphere, and the hotter and colder models (dashed grey lines) correspond to variations of ± 20 km in the thickness of the mantle lid, approximately. Also shown for comparison are the inferred temperatures and error bars from simple BHT corrections where a sequence of wireline log measurements is available from four exploration boreholes (see map for approximate locations). The temperature-depth profiles are taken at the 10 km mark on the transect (shaded arrow in e), where the stratigraphy of the uppermost 5 km is analogous to that of the wells, with less than 1 km of recent sediments, overlying approximately 2 km of Zeit-South Gharib evaporites and up to 2 km (or more) of Kareem/Rudeis syn-rift, clastic sediments. c) Predicted present-day HF at base sediments along the profile for the reference (solid black line) and end-member hotter and cooler models (dashed grey lines), corresponding to variations of ± 20 km in the thickness of the mantle lid, approximately. d) Predicted temperature structure at present-day, showing the lithosphere-asthenosphere boundary (LAB at 1300°C; dotted-dashed line) rising to <50 km depth near the rift axis. The thin grey lines are 250°C isotherms and the thin black lines are the models' horizons, including the stratigraphy and crustal structure. The inset shows the total (dark red) and Oligocene-early Miocene (light red) mantle stretching factors (δ); where the total is given by multiplying the stretching factors from the Oligocene-early Miocene passive rifting and mid/late Miocene-Present active rifting (see discussion of results). e) Modelled stratigraphy and predicted crustal structure. The modelled horizons include the seabed (0 Ma), top stratified salt (5 Ma), top mobile salt (halite; 11-12 Ma), top syn-rift (13 Ma) and acoustic basement/top pre-rift (or base syn-rift; 23 Ma), and the fit to the observed (input) stratigraphy is approximately 95% (bottom-right inset). The shaded arrow at 10 km of the model pinpoints the location of the temperature-depth profiles shown in b).

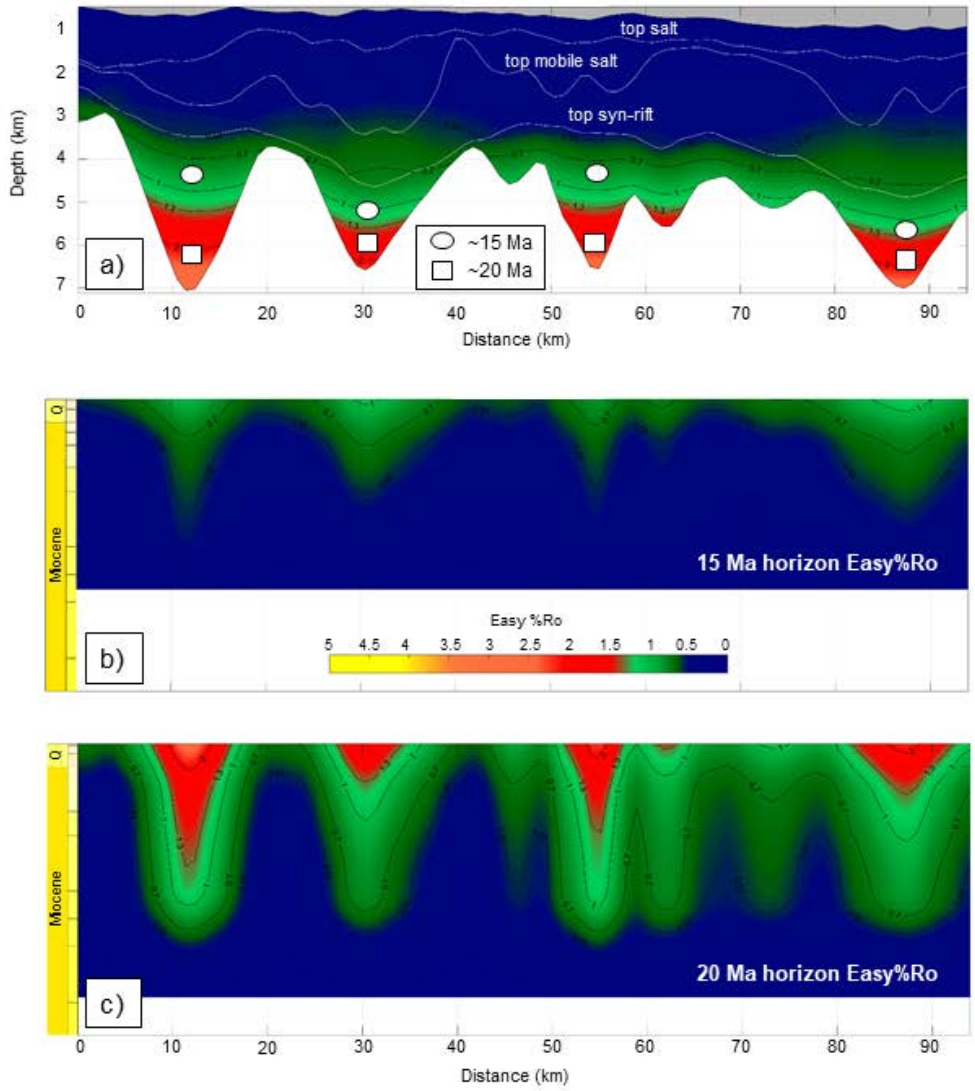

Figure 2. a) Predicted Easy%Ro vitrinite reflectance maturity (Sweeney and Burnham, 1990) for the reference model, showing the key oil and gas window markers (black lines) and the stratigraphic horizons (white lines). The colour scale reflects the commonly accepted vitrinite reflectance maturity window intervals: 0-0.5, immature (dark blue); 0.5-0.7 (dark green), early-oil mature; 0.7-1 (dark-mid green) mid-oil mature; 1-1.3 (mid-light green) late-oil to early-gas mature; 1.3-2.2 (red) gas mature; 2.2-3 (orange) late-gas mature; >3 (orange-yellow) post-mature. The ovals and squares show the approximate depths of the 15 Ma and 20 Ma horizons in the sub-basins, for which the maturity history is shown in b) and c), respectively. b-c) Predicted Easy%Ro vitrinite reflectance maturity through time for two horizons within the syn-rift section, at 15 and 20 Ma.